10B.3 EFFECTS OF THE MADDEN_JULIAN OSCILLATION ON THE CYCLOGENESES OF HURRICANE FAUSTO (2002) AND HURRICANE EMILY (2005)

Stephanie E. Zick* and William M. Frank
Pennsylvania State University, University Park, PA

1. INTRODUCTION

The necessary climatological conditions for tropical cyclogenesis are generally agreed upon and can be summarized as sea surface temperatures above 26.5°C overlaying a deep oceanic mixed-layer, deep convection within a region of moist lower and middle levels, positive low-level vorticity anomalies, and weak (or slightly easterly) vertical wind shear (Gray 1968, 1979). While the climatological conditions are well-known, these conditions exist over a large portion of the tropics for extended time periods. Only a small percentage of potential disturbances develop into tropical storms. This suggests that there must be additional criteria for individual storms.. Despite the availability of advanced global observations and high-resolution numerical models, the local conditions necessary for genesis remain somewhat of an enigma.

Tropical cyclones form within pre-existing convective regions which are often embedded in synoptic-scale cyclonic regions such as monsoon troughs, tropical waves, or cyclonic frontal disturbances that move equatorward into the tropics. These cyclonic regions are on a scale much larger than a tropical cyclone core. One theory is that tropical waves make the local environment more favorable for genesis. Frank and Roundy (2006) showed that the Madden-Julian Oscillation (MJO), equatorial Rossby waves, and tropical depression type (TD-type) waves (such as African easterly waves) play significant roles in the development of many cyclones every year in all six major basin. The goal of this research is to investigate how the MJO affects tropical cyclogenesis using the Weather Research and Forecast (WRF) model version 2.2 (WRFV2.2) and real data.

2. PREVIOUS STUDIES

Weather in the tropics is principally modulated by disturbances that propagate parallel to the equator, i.e. equatorial waves. These disturbances modify the background flow by perturbing the large-scale vertical velocity, low-level and upper-level vorticity, and vertical wind shear fields. With the advent of the satellite era and the consequent availability of global datasets, it became possible to study organized convection in the tropics in terms of the dominant wavenumbers and frequencies via spectral analysis of outgoing longwave radiation (OLR) and brightness temperature. Wheeler and Kiladis (1999) identified the prominent convectively-couple equatorial wave types using wavenumber-frequency analysis of OLR: Kelvin, equatorial Rossby (ER), mixed Rossby-gravity (MRG), eastward inertio-gravity (EIG), westward inertio-gravity (WIG) waves., the Madden-Julian Oscillation (MJO) and tropical depression-type waves (TD-type, also known as African easterly waves).

Roundy and Frank (2004) conducted a climatology of the five dominant convectively-coupled wave types in the equatorial region: the MJO, equatorial Rossby waves, mixed Rossby-gravity waves, Kelvin waves, and TD-type disturbances. Using Fourier filters to separate the time-longitude components for each of the five spectral bands, they found that the MJO and equatorial Rossby waves account for more than 15% of the variance in total OLR and more than 50% in local OLR in the tropics. Since OLR is correlated with convection, these waves significantly affect tropical weather. This paper focuses on how tropical cyclones interact with the MJO, which was discovered by Madden and Julian in 1971.

Hendon and Salby (1994) discussed the MJO life cycle. This cycle begins with enhanced convection over the Indian Ocean and reduced convection over the western Pacific, generally favoring the summer hemisphere (Roundy and Frank, 2004). The region of enhanced convection is related to convergence at 850mb and divergence at 200mb. The MJO then propagates eastward at a phase speed of about 5 ms^{-1} when convection is strong and about 10 ms^{-1} when convection is weak (Hendon and Salby, 1994). While its signal is most evident in the Indian and Pacific Oceans, the circulation affects the entire tropical troposphere.

Using spectral analysis and filtering for each of the five dominant wave types in the equatorial region, Frank and Roundy (2006) created composite analyses of wave fields with respect to genesis location in each basin. About 60-70 %of tropical cyclogenesis cases occurred within the negative MJO-filtered OLR anomalies in each of the six basins. In the East Pacific, cyclogenesis in the

* Corresponding author address: Stephanie E. Zick, Department of Meteorology, Penn State University, 503 Walker Building, University Park, PA 16802; e-mail: sez113@psu.edu.

composites occurred on the poleward edge of the MJO-filtered westerly wind anomaly and on the leading edge of the eastward propagating low-level cyclonic vorticity anomaly. This corresponded with a peak in MJO-filtered OLR anomalies. Similar features were found in the North Atlantic for MJO-filtered fields; however, these features were less prominent in the North Atlantic. The MJO also reduced westerly vertical wind shear prior to cyclogenesis in all basins, which is known to inhibit tropical cyclone intensification (Frank and Ritchie, 2001).

Several recent studies have investigated the interaction between the MJO and tropical cyclones in the East Pacific. Moliari et. al. (1997) and Molinari and Vollaro (2000) proposed that the MJO entered the East Pacific and Caribbean Sea, enhancing convection in these regions. Positive potential vorticity (PV) anomalies then amplified in the east Pacific along the ITCZ and over northern South America, leading to an intensification of the meridional PV sign reversal. During this time period, waves were able to grow on the unstable background state and cyclogenesis was much more frequent. Maloney and Hartmann (2000) saw that tropical cyclones were four times more likely to form when 850 hPa wind anomalies were westerly. Cyclones also became more intense in westerly periods. Dynamical aspects contributing to increased basin activity were increased cyclonic horizontal shear and low vertical wind shear, both of which are conducive to uurricane formation and intensification. A follow-up study by Maloney and Hartmann (2001) examined the role of barotropic dynamics in the eastern Pacific and demonstrated that eddies grow via barotropic eddy kinetic energy (EKE) conversion when 850 mb zonal wind anomalies are westerly.

3. METHODS

This section outlines the methodology used in this study. We first apply spectral analysis to determine the phase of the MJO during genesis and intensification. This research takes advantage of the WRF model (section 3.2). Control simulations of both case studies are run; the initial conditions then are perturbed by removing an idealized representation of the MJO. The statistical technique applied to remove the MJO from the initial conditions is described in section 3.3. An ensemble, elaborated on in section 3.4, of each case study is run for statistical robustness.

3.1 *Spectral Analysis*

The diagnostic analysis involves filtering National Centers for Environmental Prediction/National Center for Atmospheric Research (NCEP/NCAR) reanalysis wind and OLR for the MJO. The filter used in this study is for periods of 30-100 days and wavenumbers of 0-10. The filtered fields are studied on a longitude-time grid to diagnose MJO convectively active and convectively inhibitive phases. In addition, the filtered OLR anomaly and zonal wind anomalies are plotted on a latitude-longitude grid just prior to and just after tropical cyclone intensification. Synoptic scale features are also considered in relation to cyclone development.

3.2 *The WRF Model*

WRFV2.2 program code was developed collectively by researchers at the National Center for Atmospheric Research (NCAR), the National Oceanic and Atmospheric Administration, the National Centers for Environmental Prediction (NCEP) the Forecast Systems Laboratory (FSL), the Air Force Weather Agency (AFWA), the Naval Research Laboratory, Oklahoma University, and the Federal Aviation Administration (FAA). Complete documentation on the WRF model

The WRF model solves the fully compressible, nonhydrostatic Euler equations using a mass-based terrain-following vertical coordinate. All scalar variables are conservative. A 3rd order Runge-Kutta time-split integration scheme is employed with smaller timesteps for acoustic and gravity-wave modes (Skamarock et al., 2005). WRF is highly modular; various model physics parameters can be specified by the user. Section 3.4 will further address the physics options used in this study.

First, we perform control simulations for each case. The coarse domain in this study is 54 km horizontal grid spacing with nests of 18 km and 6 km. All simulations are run with 29 vertical levels. Initial conditions are created by horizontal interpolation NCEP final analysis data to the 54 km grid and then vertically interpolating to the terrain-following coordinate. Thus, a hydrostatically balanced 3D grid is created as input to the WRF model (Skamarock et. al., 2005).

For real data cases, WRF specifies the horizontal boundary conditions by a method often referred to as a relaxation of a nudging. Boundary conditions at the top of the model are constant pressure with a vertical velocity of zero. (Skamarock et. al. 2005). Nesting in the smulations is one way, so the only communication with the nested grid is through its boundary conditions, which are interpolated from the parent grid. These lateral boundary conditions are provided at each coarse grid time step.

3.3 *Modification of Initial Conditions*

After performing a control run for each case, the filtered wave anomaly field is removed from the initial conditions. The cases then are rerun. By comparing the simulations, the effects of the MJO on the simulated storm can be determined. Initial conditions are modified by running a linear

regression for five years of input data versus an EOF time series of the idealized tropical wave. These EOF time series, calculated using spectral analysis to filter OLR anomalies, were created by Dr. Paul E. Roundy at the University of Albany (personal communication). EOF analysis then is applied to those anomalies, and the OLR anomalies are projected onto the first 75 EOFs, which account for 90% of the variance. The atmospheric wave is removed by subtracting the correlated part for each input at each gridpoint.

This procedure is a new technique and an idealized approach to removing the MJO wave field. A simulation that is initialized with actual observations is chosen because it allows verification of the model results. By comparing the results of these simulations to the control run we will estimate the effects of the MJO upon the real storm.

3.4 *Ensemble Technique*

Owing to the newness of the procedure, the case studies are runs as ensembles to ensure that the results are statistically significant. Five ensemble members are created by varying the microphysical and cumulus parameterizations. This is outlined in Table 1. The C denotes control simulations, and the M denotes MJO-removed simulations. Modeling of tropical cyclones is known to be highly sensitive to physical processes (e.g. Puri and Miller 1990; Braun and Tao 2000; Davis and Bosart 2002). This study employs two convective parameterization schemes, the Betts-Miller-Janjic scheme (hereafter BMJ) and the Kain-Fritsch Eta scheme (hereafter KF). Convective parameterizations attempt to represent the unresolved vertical fluxes due to convective updrafts and downdrafts. Theoretically, convective parameterizations should only be applied at at coarse grid resolutions: in the 5-10 km horizontal grid spacing range, the model begins to resolve some convection explicitly. Therefore, a fifth ensemble member is initialized with the coarse grid of ensemble member 1 and run with fully explicit convection.

	Microphyics Scheme	Cumulus Parameterization
CEM1/MEM1	WSM6	KF
CEM2/MEM2	WSM6	BMJ
CEM3/MEM3	Eta	KF
CEM4/MEM4	Eta	BMJ
CEM5/MEM5	WSM6	Fully explicit

Table 1. Description of Ensemble Members

Microphysical parameterizations are also varies within the ensemble. The WRF Single-Moment 6 class scheme (herafter WSM6) and the Eta microphysics scheme (also known as the Eta Ferrier scheme) are used in this study. All simulations are run using the Yonsei University (YSU) planetary boundary layer scheme, the Rapid Update Cycle (RUC) model land surface model, the Rapid Radiative Transfer Model longwave radiation scheme, and the Dudhia shortwave radiation scheme.

4. RESULTS

Two case studies are considered: Hurricane Fausto from the 2002 East Pacific season and Hurricane Emily from the 2005 North Atlantic season. Hurricane Fausto formed during a convectively active phase of the MJO, whereas Hurricane Emily formed during a more neutral MJO environment. A comparison of control and MJO-removed simulations for each case study follows.

4.1 *Hurricane Fausto (2002)*

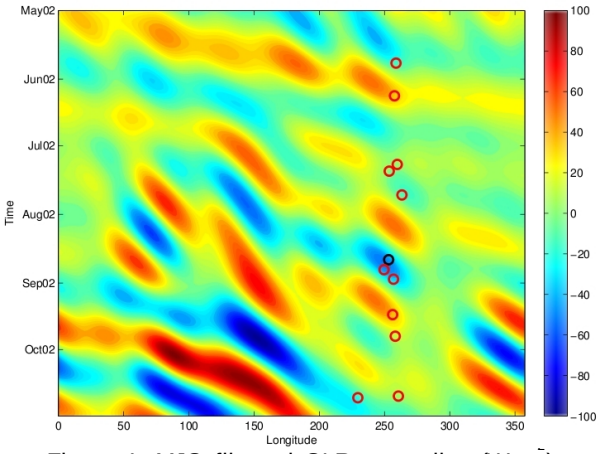

Figure 1. MJO-filtered OLR anomalies (Wm ¯) averaged over 0-20°N. Circles represent genesis locations for all named storms in the east Pacific basin in 2002. Hurricane Fausto is denoted by the black circle.

Previous to the development of Hurricane Fausto, more than three weeks had elapsed with no named storms in the northeast Pacific basin. Figure 1 displays longitude-time plots, i.e., Hövmollers, of MJO-filtered OLR anomalies as well as the locations of development of all named storms in the northeast Pacific for the period May-October 2002. The OLR anomalies are calculated by subtracting the long-term mean of daily OLR from daily OLR data at each location. These anomalies then are filtered for the MJO and are averaged over the tropical Northern Hemisphere between the equator and 20°N. Warm colors indicate that MJO-filtered OLR anomalies are

above average (convection is reduced) while cold colors indicate that the anomalies are below average (convection is enhanced). Hurricane Fausto led the way into an active period for the northeast Pacific basin; Tropical Storm Genevieve and Hurricane Hernan also formed at the end of August within a convectively favorable region of MJO-filtered OLR anomalies.

To determine the performance of the linear regression used to modify the initial conditions, the difference fields in initialized 850 mb and 200 mb winds (control minus MJO-removed) are shown in Figures 2a and 2b, respectively. These wind fields were subtracted from the initial conditions to create the MJO-removed simulations. Hurricane Fausto formed within an MJO-filtered 850 mb easterly wind anomaly (not shown). The cyclone then moved into a region of low-level convergence related to the intersection of westerly and easterly wind anomalies associated with the MJO.

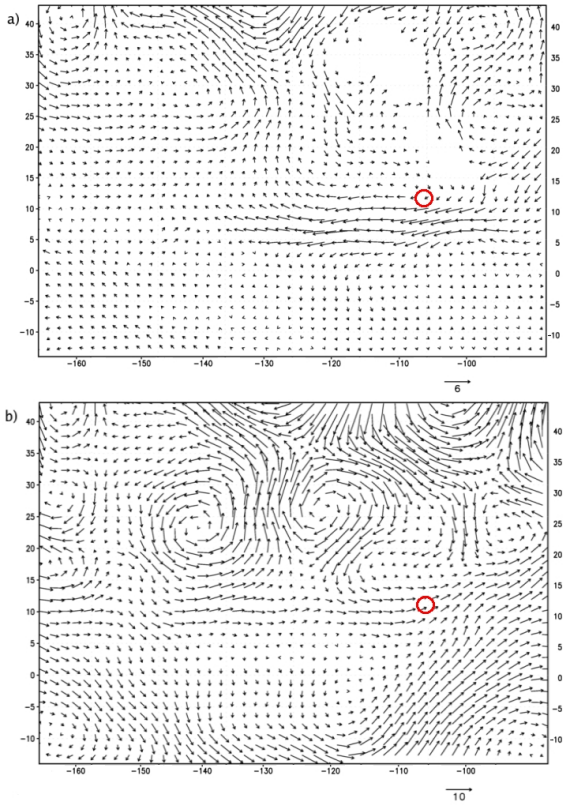

Figure 2. Initial 850 mb and 200 mb wind (ms^{-1}) difference field (control minus MJO-removed) for 54km domain. The red circle indicates the approximate location of Hurricane Fausto at this time.

From Figure 2a, it is also evident that a meridional component of the 850 mb wind was removed from the initial conditions in some portions of the domain. The MJO generally is not believed to have a strong meridional component; however, some studies have observed northward propagating cloud zones to 30°N in the Indian monsoon (Madden and Julian, 1994). Most of the north-south flow subtracted from 850 mb initial winds is confined to the portion of the coarse domain that lies in the extratropics. In the extratropics, effects of the MJO are not well understood. Some global models predict a 50 day oscillation in angular momentum. Other studies have revealed 40-50 day variations in angular momentum, geopotential height, and winds, but any connection between these observations and the MJO is at this point tenuous (Madden and Julian, 1994).

Considering Figure 2b, a 200 mb westerly wind was removed from the initial conditions in the vicinity of the storm. Hurricane Fausto formed during a transition from westerly MJO-filtered 200 mb wind anomalies to easterly MJO-filtered 200 mb winds. Upper-level easterly wind anomalies are associated with the convectively active phase of the MJO, whereas upper-level westerly wind anomalies are associated with the convectively inhibitive phase of the MJO. An in-depth comparison of the results of methodology used to remove the MJO is not presented here. However, the circulations that were removed from the initial conditions are determined to agree well with MJO-filtered wind fields at that time.

Tracks of the location of minimum SLP for each 6 km resolution ensemble member are displayed in Figure 3. It is important to note that storm tracks are not of equal lengths because the cyclones in some simulations weakened, resulting in undetectable centers. From this figure, two features are immediately clear. First, the location of minimum SLP for control simulations and MJO-removed simulations at the time of initialization of the 6 km resolution domain are distinctly offset. In addition, the cumulus parameterization had a marked effect on storm track. Previous studies (e.g. Davis and Bosart 2002) have found that choice of cumulus parameterization strongly affects storm track and intensity.

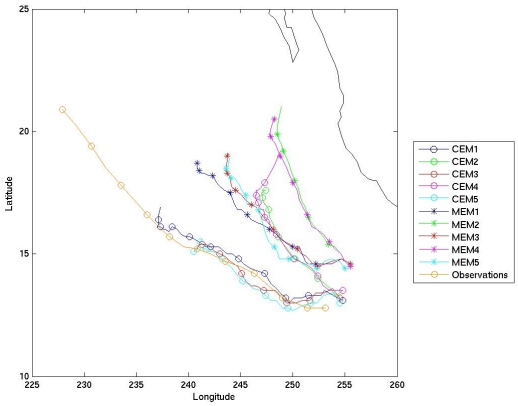

Figure 3. Tracks of minimum SLP for 6 km ensemble members. Tracks are marked every 12 hours with circles

(asterisks) for control (MJO-removed) simulations beginning at 00Z Aug 21

Due to the modification of the initial wind fields, all MJO-removed simulations form the cyclone to the northeast of all control simulations. The modification in the initial wind field transfers the region of low-level relative vorticity anomaly to the north-northeast, as shown in Figure 4. This figure also clearly shows the monsoon trough, which Hurricane Fausto formed within. In the MJO-removed simulation, the monsoon trough takes on a more northeasterly tilt, and the cyclone forms to the northeast of the control simulation. This initial location shift results in significant differences in the evolving storm intensities. Differences in initial locations of the control and MJO-removed ensemble mean minimum SLP are much larger than one standard deviation in latitude and longitude. Therefore, in the case of Hurricane Fausto, a statistically significant difference in storm track is observed when the MJO is removed from the initial conditions.

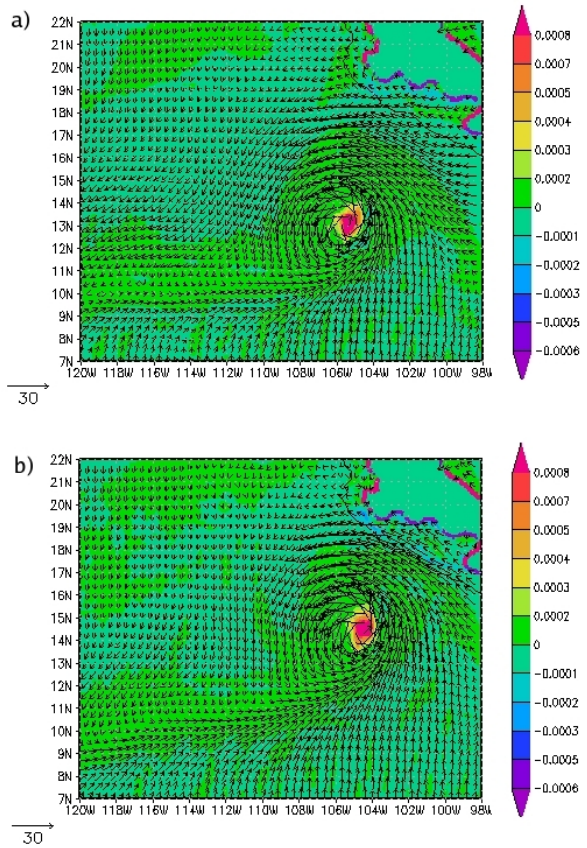

Figure 4. Comparision of a) CEM1 and b) MEM1 850mb relative vorticity s^{-1}) and 850 mb winds (ms^{-1}) at 00Z Aug 21

Due to diverging storm tracks, each simulation of Hurricane Fausto encounters varying synoptic conditions. Minimum SLP versus time for each ensemble member, the ensemble means, and observations are shown in Figure 5. It is hypothesized that the WRF model does a poor job of simulating the observed intensity of Hurricane Fausto because of uncertainty in the initial conditions. Observations are sparse over the eastern and central Pacific, which can negatively affect the performance of NWP models and modeling studies.

The differences in storm intensity between simulations can be partially explained by differing storm tracks. Both VWS and SST were calculated by averaging values within a radius of 4° of the location of minimum SLP. The cyclone MEM1 tracks over cooler SSTs into a region of stronger vertical wind shear (not shown). Likewise, for each respective ensemble member, the MEM simulation tracks farther north into a less favorable environment than does the corresponding CEM simulation. In the MEM1 simulation, an increase to nearly 30 ms^{-1} of total VWS is followed by a period of dramatic weakening. Meanwhile, the CEM1 simulation maintained its intensity under about 25 ms^{-1} of total VWS. Because the MJO-removed simulations formed in a different location than the control simulations, the MJO indirectly affected the the evolutions of the simulated storms and the subsequent tracks of the storms. When comparing control and MJO-removed simulations run with the same physics, each control storm is more intense on at least a 99% confidence level.

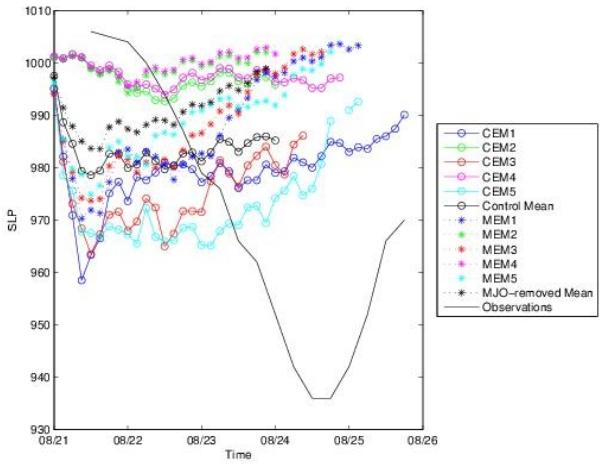

Figure 5. Timeseries of minimum SLP (mb) for 6 km ensemble members, ensemble mean, and observations. Circles (asterisks) designate control (MJO-removed) simulations.

4.2 *Hurricane Emily (2005)*

Hurricane Emily was the fifth named storm of the 2005 Atlantic hurricane season. One of seven major hurricanes in the record-breaking 2005 season, Hurricane Emily intensified to a minimum pressure of 929 mb before making landfall as a

category 4 hurricane on the Yucatan peninsula. Hurricane Emily formed over the central Atlantic Ocean from an African easterly wave. Based on MJO-filtered OLR and wind anomalies, the influence of the MJO on the genesis and intensification of Hurricane Emily was weak to nearly neutral. However, some subtle influences may be observed, and it is useful to compare the case study of Hurricane Emily to the case study of Hurricane Fausto.

Hurricane Emily developed (was classified as a depression) during a weakly inhibitive phase of the MJO. Emily reached hurricane strength at 00Z Jul 14 during a time when the MJO-filtered OLR and 850 mb zonal winds were weakly favorable for convection and, therefore, cyclogenesis. Unlike Hurricane Fausto, control and MJO-removed simulated storms formed in the same location. The simulated storms were also more similar with respect to intensity. However, in both case studies, the large-scale vertical wind shear was most significantly modified when the MJO was removed from the initial conditions.

5. CONCLUSIONS

There are several conclusions that can be drawn from the research presented in this paper:

1) A 6 km resolution WRF simulation can capture variations in location and orientation of the ITCZ and monsoon trough. For the case study of Hurricane Fausto, the monsoon trough and its associated low-level relative vorticity were displaced to the north when the MJO was removed from the initial conditions.

2) The MJO caused significant variation in VWS. These variations affected the genesis location and intensification of the simulated storms. Therefore, numerical weather prediction models must be able to model circulations such as the MJO to accurately predict the timing and location of cyclogenesis and the subsequent intensification of the cyclone.

3) The WRF model is able to simulate sensitivity of tropical cyclogenesis to to VWS. In both of the case studies of Hurricane Emily and Hurricane Fausto, the simulated storms were highly sensitive to VWS.

4) A multiple linear regression of the first PCs of a wave field versus a time series of GFS final analysis data can be used to remove the correlated components of that wave from the GFS final analysis data used to initialize a model. This was verified by good agreement between MJO-filtered wind anomalies and the calculated MJO-correlated components of the initial analysis field for the case of Hurricane Fausto.

5) Based on the performance of the methodology used to remove the MJO from the initial conditions, the MJO was more prevalent in the initial fields in the east Pacific case study of Hurricane Fausto than in the central Atlantic case study of Hurricane Emily. Whether this is because the MJO is weaker in the central Atlantic cannot be determined since only two cases were studied.

6. REFERENCES

Davis, C. A., and L. F. Bosart, 2002: Numerical simulations of the genesis of Hurricane Diana (1984). Part II: Sensitivity of track and intensity prediction. *Mon. Wea. Rev.,* **130,** 1100-1124.

Frank, W. M., and P. E. Roundy, 2006: The role of tropical waves in tropical cyclogenesis. *Mon. Wea. Rev.*, **134**, 2397—2417.

Frank, W. M., and E. A. Ritchie, 2001: Effects of vertical wind shear on the intensity and structure of numerically simulated hurricanes. *Mon. Wea. Rev.*, **129**, 2249-2269.

Gill, A. E., 1982: *Atmosphere-Ocean Dynamics*, Academic Press, 662 pp.

Hendon, H. H., and M. L. Salby, 1994: The life cycle of the Madden-Julian Oscillation. *J. Atmos. Sci.*, **51**, 2225-2237.

Holton, J. R., 1992: *An Introduction to Dynamics Meteorology*, Academic Press, 511 pp.

Madden, R. A., and P. R. Julian, 1994: Observations of the 40-50 day tropical oscillation--A review. *Mon. Wea. Rev.*, **122**, 814--837.

Maloney, E. D., and D. L. Hartmann, 2000b: Modulation of eastern North Pacific hurricanes by the Madden-Julian Oscillation. *J. Climate.*, **13**, 1451--1460.

Maloney, E. D., and D. L. Hartmann, 2001: The Madden-Julian Oscillation, barotropic dynamics, and North Pacific tropical cyclone formation, Part I: observations. *J. Atmos. Sci.*, **58**, 2245--2558.

Molinari, J. et al., 1997: Potential vorticity, easterly waves, and Eastern Pacific tropical cyclogenesis. *Mon. Wea. Rev.*, **125**, 2699--2708.

Molinari, J., and D. Vollaro, 2000: Planetary- and synoptic-scale influence on Eastern Pacific tropical cyclogenesis. *Mon. Wea. Rev.*, **128**, 3296--3307.

Roundy, P. E., and W. M. Frank, 2004a: A climatology of waves in the equatorial region. *J. Atmos. Sci.*, **61**, 2105—2132.

Skamarock, W. C., J. B. Klemp, J. Dudhia, D. O. Gill, D. M. Baker, W. Wang and J. G. Powers, 2005: A description of the advanced research WRF version 2. NCAR/TN-468+STR, 88pp.